The NA60 Silicon Vertex Spectrometer

Károly Banicz

on behalf of the NA60 collaboration

Physics Goals

- Study extremely hot and dense matter (as in the early Universe)
  - by colliding heavy nuclei at ultrarelativistic energies
  - and analyzing the spectrum of the produced dimuons.
- QCD: phase transition above a critical temperature or energy density from hadronic matter to a state of deconfined quarks and gluons (Quark Gluon Plasma)

To see if…	observe…	by…	This requires…
chiral symmetry is restored,	changes in the shape of ρ	resolving resonances at different collision centralities.	good momentum resolution and high statistics.
thermal equilibrium is reached,	thermal dimuons	distinguishing them from displaced charm decay dimouns.	excellent vertexing precision.
charmonia ($c\bar{c}$) are dissolved,	their suppression with increasing centrality	counting them at different collision centralities.	high statistics and centrality measurement.

Objectives and Requirements

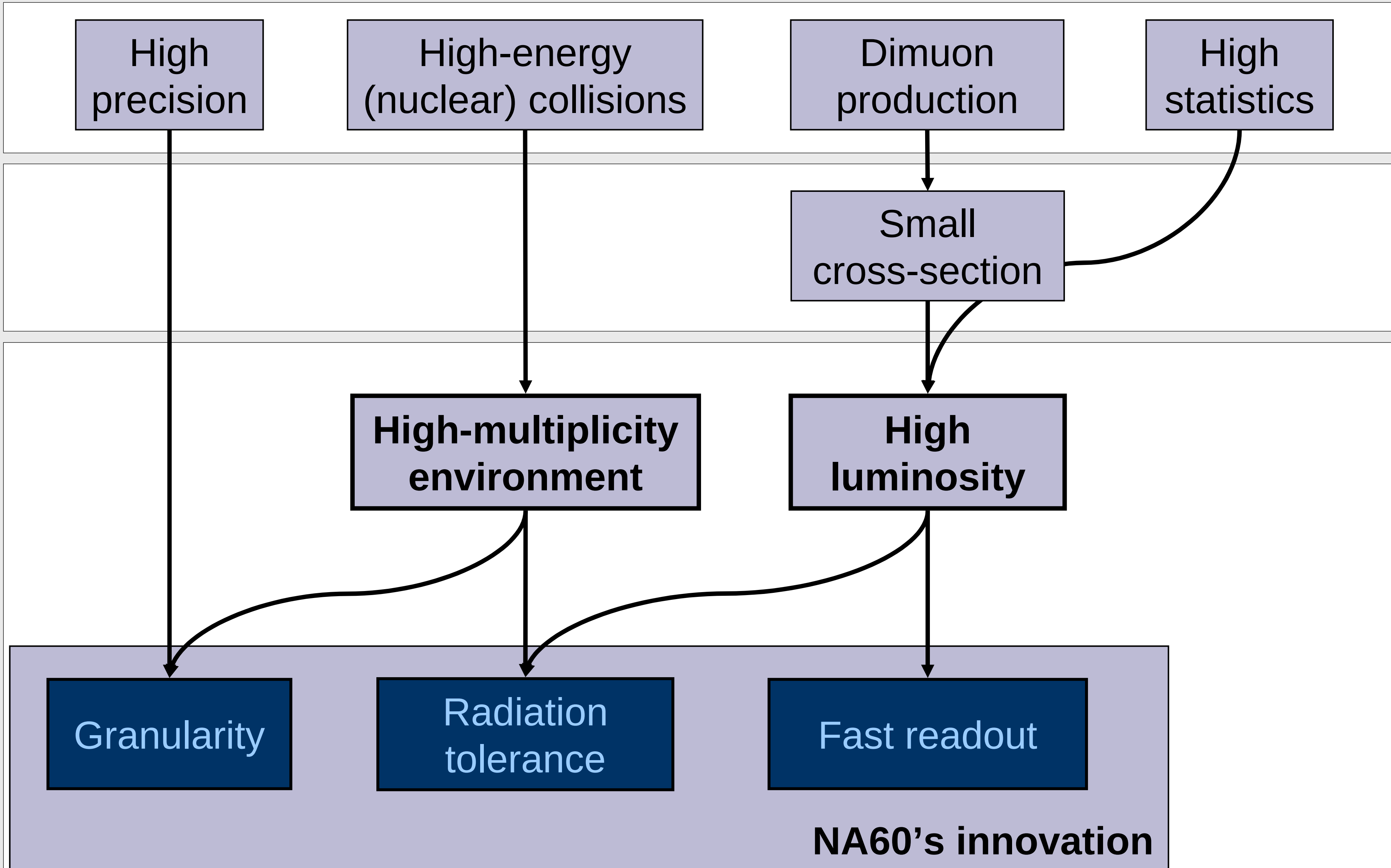

Measuring Dimuons in the Target Region

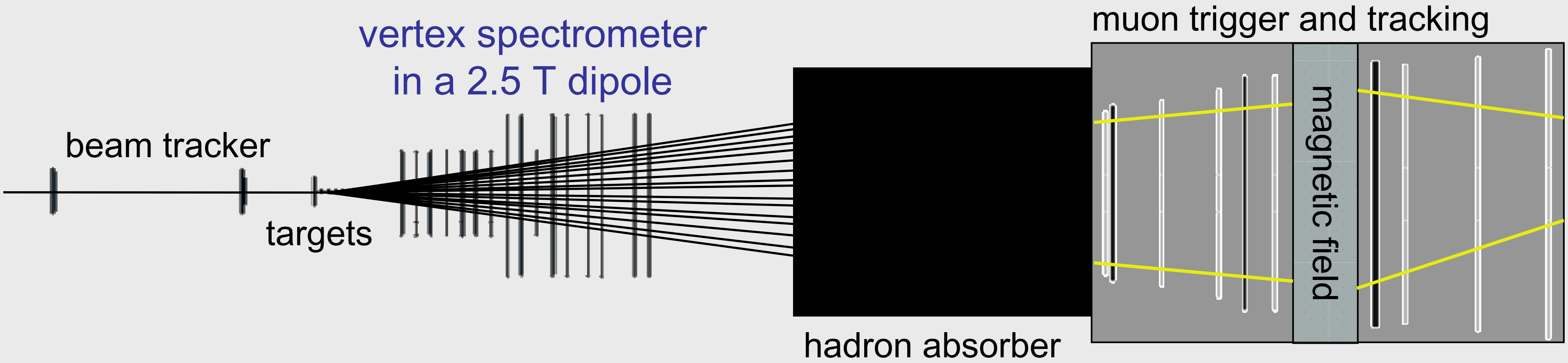

Measuring Dimuons in the Target Region

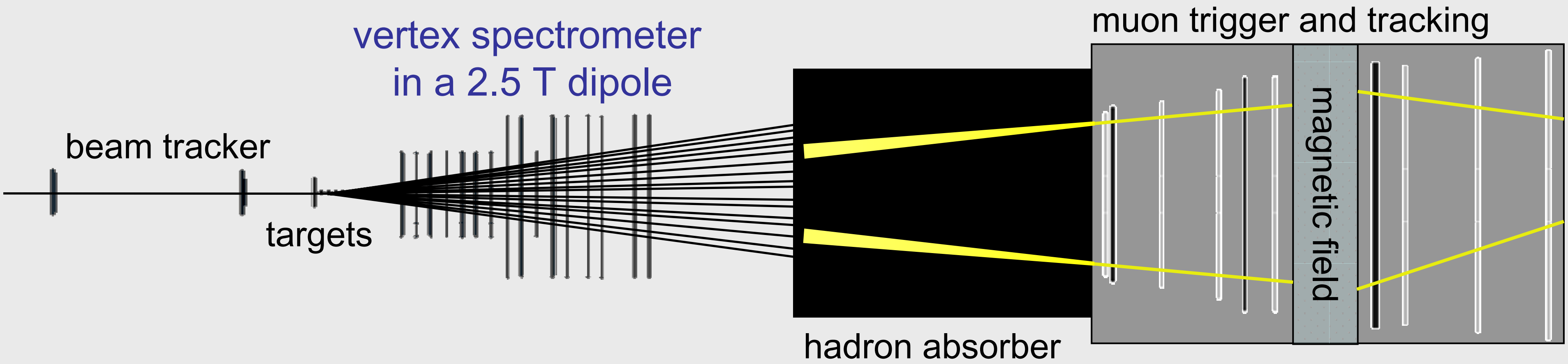

Measuring Dimuons in the Target Region

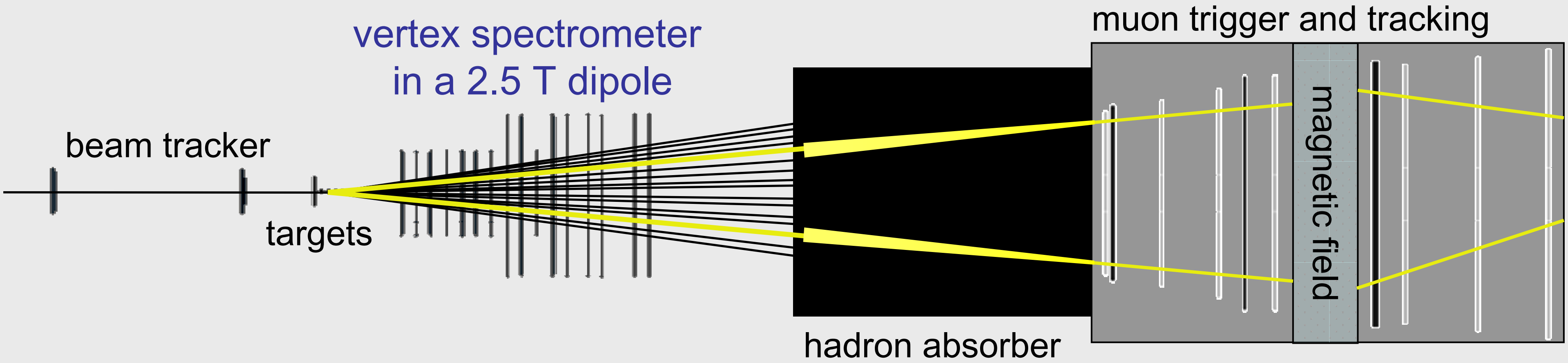

Matching in coordinate and momentum space

Origin of muons can be accurately determined

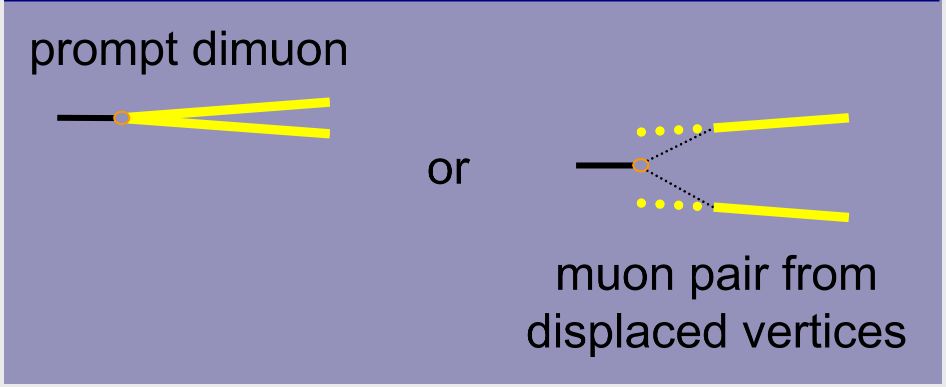

Improved dimuon mass resolution

The Silicon Vertex Spectrometer

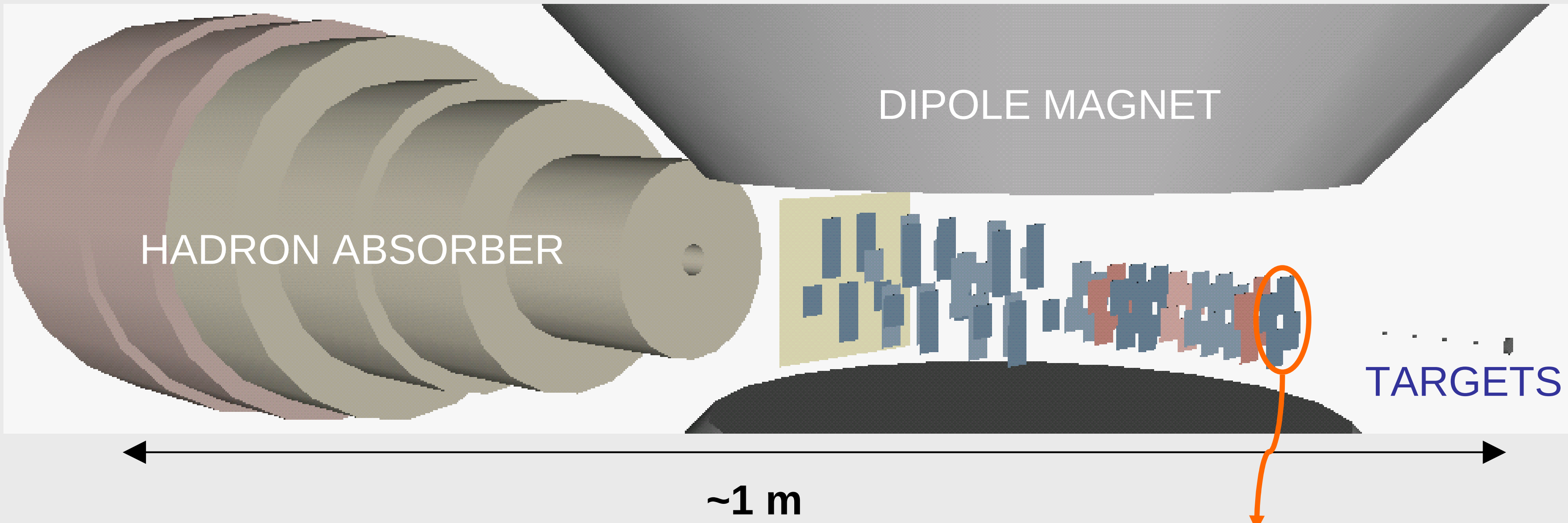

- eight 4-chip planes
- eight 8-chip planes
  (two for one space point)
- 11 space points for tracking
- inside a 2.5 T dipole magnet
- chips on ceramic hybrid

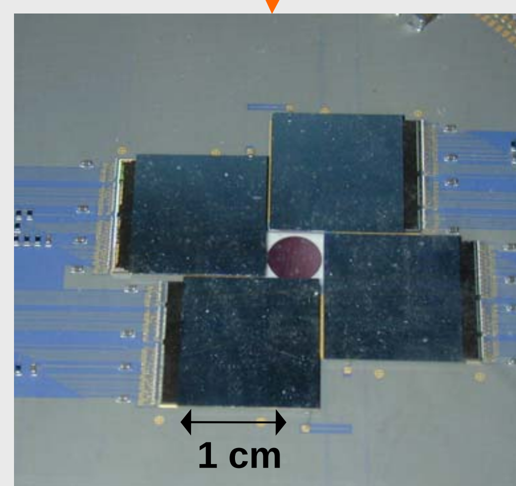

The Readout Chip

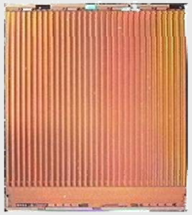

- 750 µm thick
- 32 × 256 pixels of 425 µm × 50 µm
- operated at 10 MHz
- 32 columns read out in parallel
- radiation tolerant architecture
- designed for ALICE and LHCb by CERN Microelectronics Group

The Sensor Chip

- 300 µm thick
- 32 × 256 pixels of 425 µm × 50 µm
- p implants on n bulk

Bump-bonded together

with 25 µm solder bumps

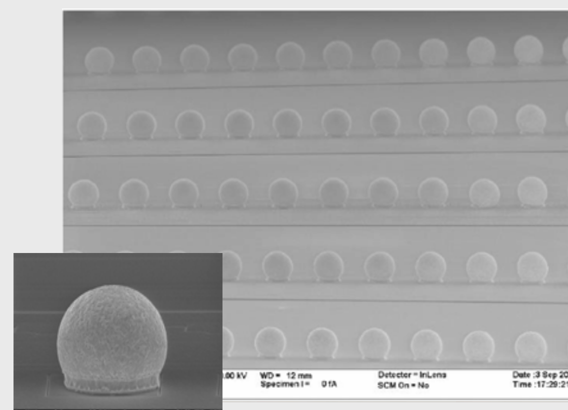

The Silicon Vertex Spectrometer

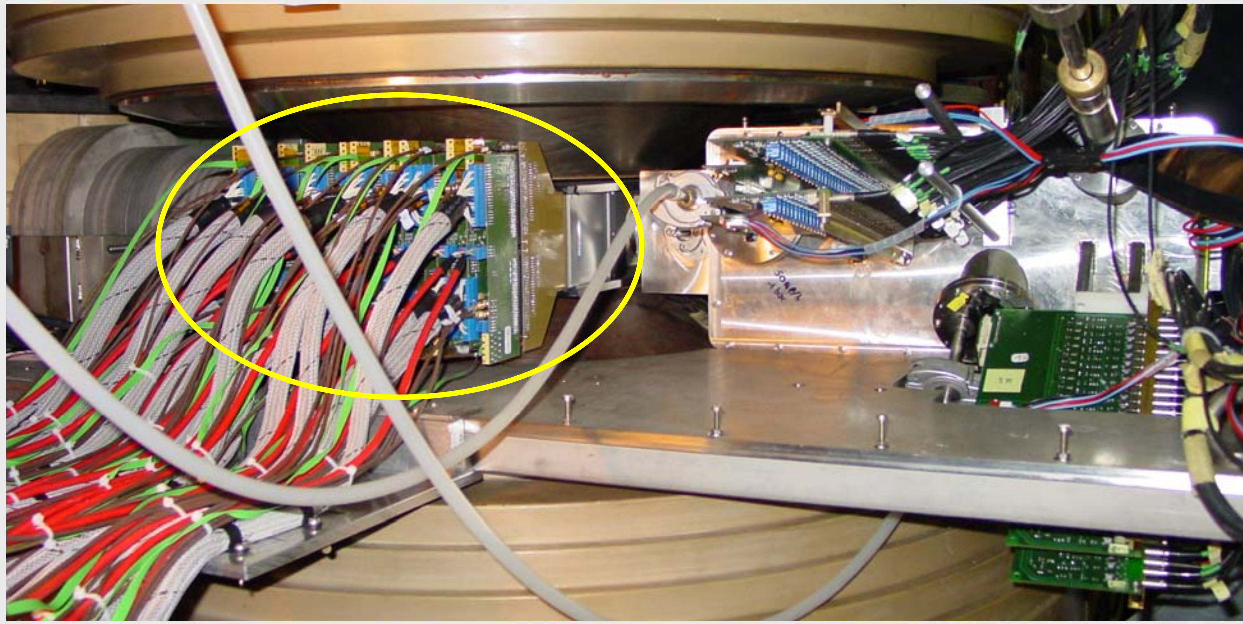

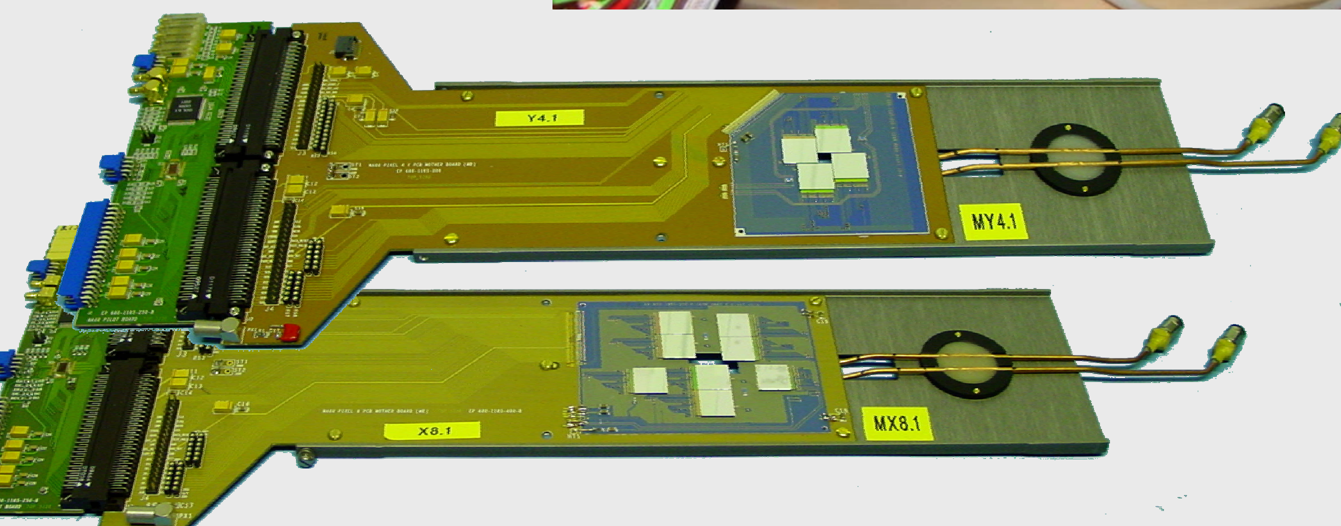

×8

×8

Pixel Telescope Vertexing

Data collected in October 2003 with 158 GeV Indium beam

Z-vertex
determination
from pixel telescope

σ_z = 300 µm

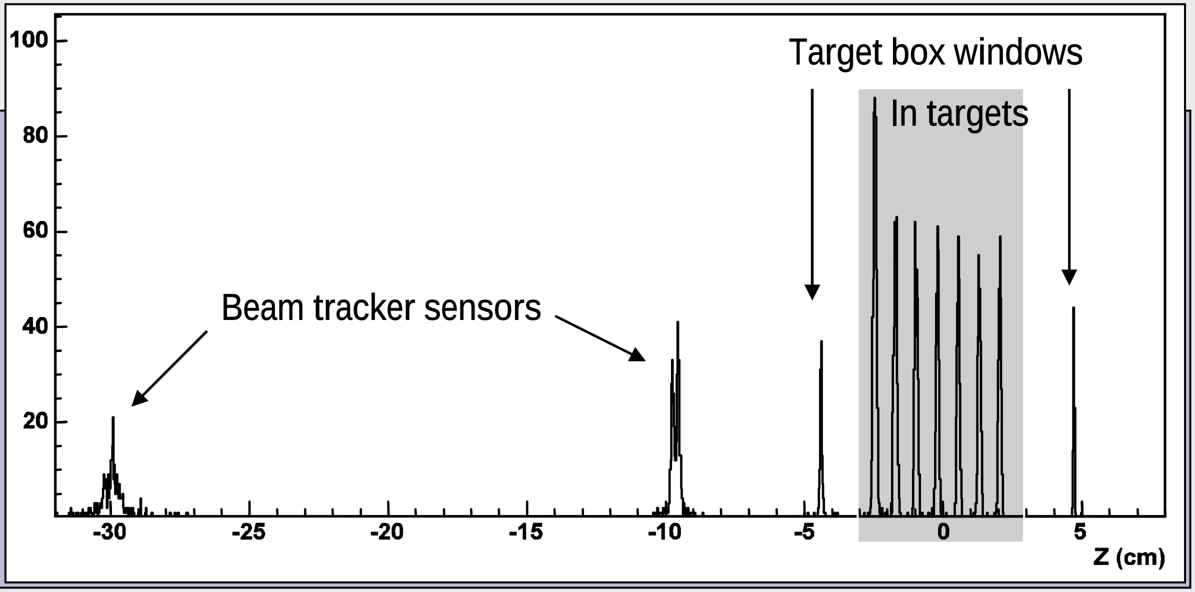

Transverse coordinates
measured
by the pixel telescope
and the beam tracker

σ_{bt} ~ 20 µm → σ_{pt} ~ 18 µm

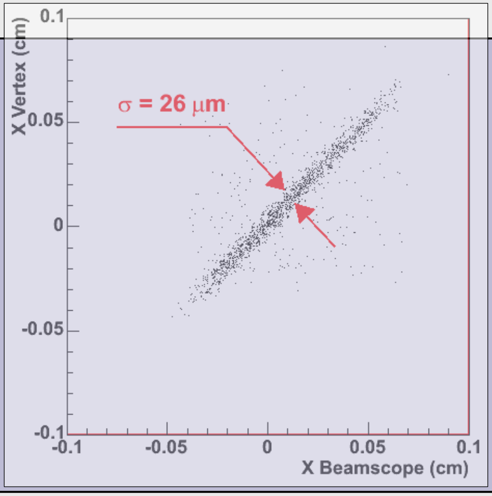

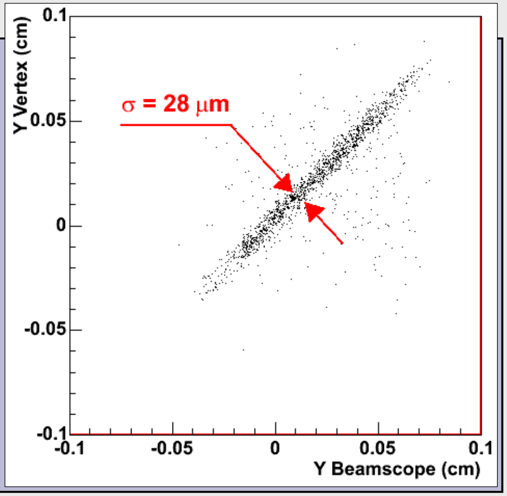

Dimuon Mass Spectrum in Indium-Indium Collisions

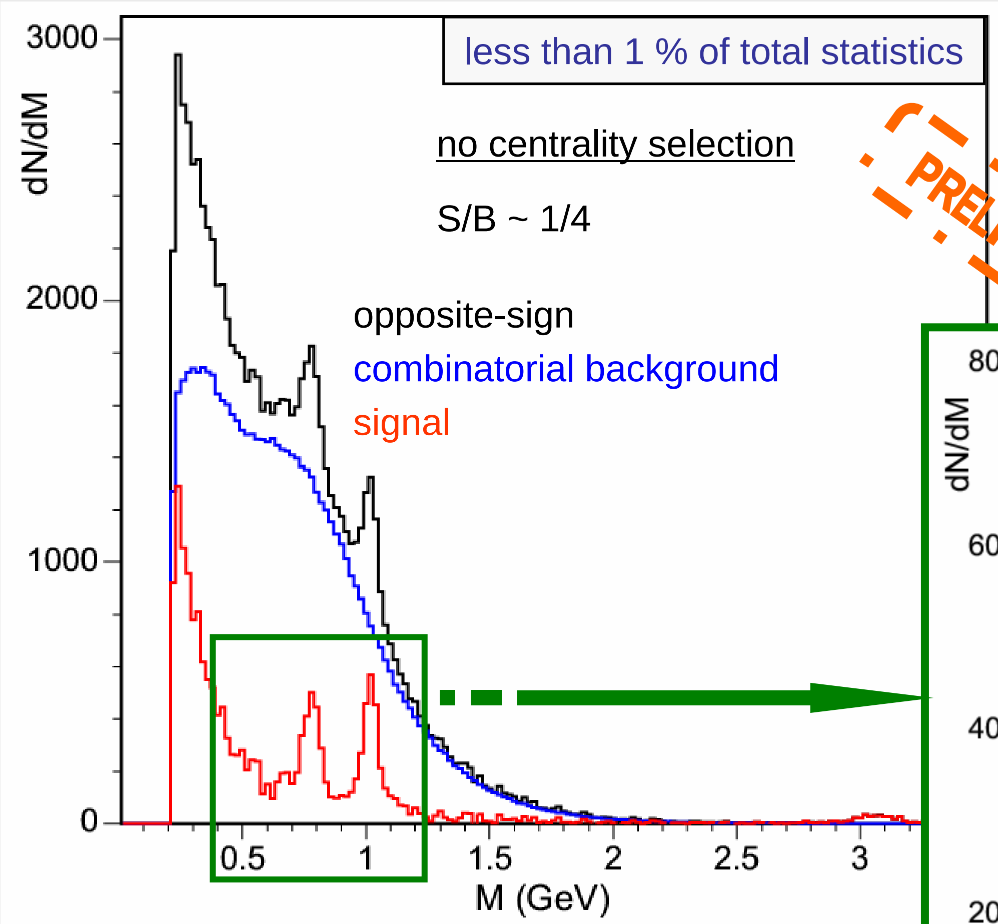

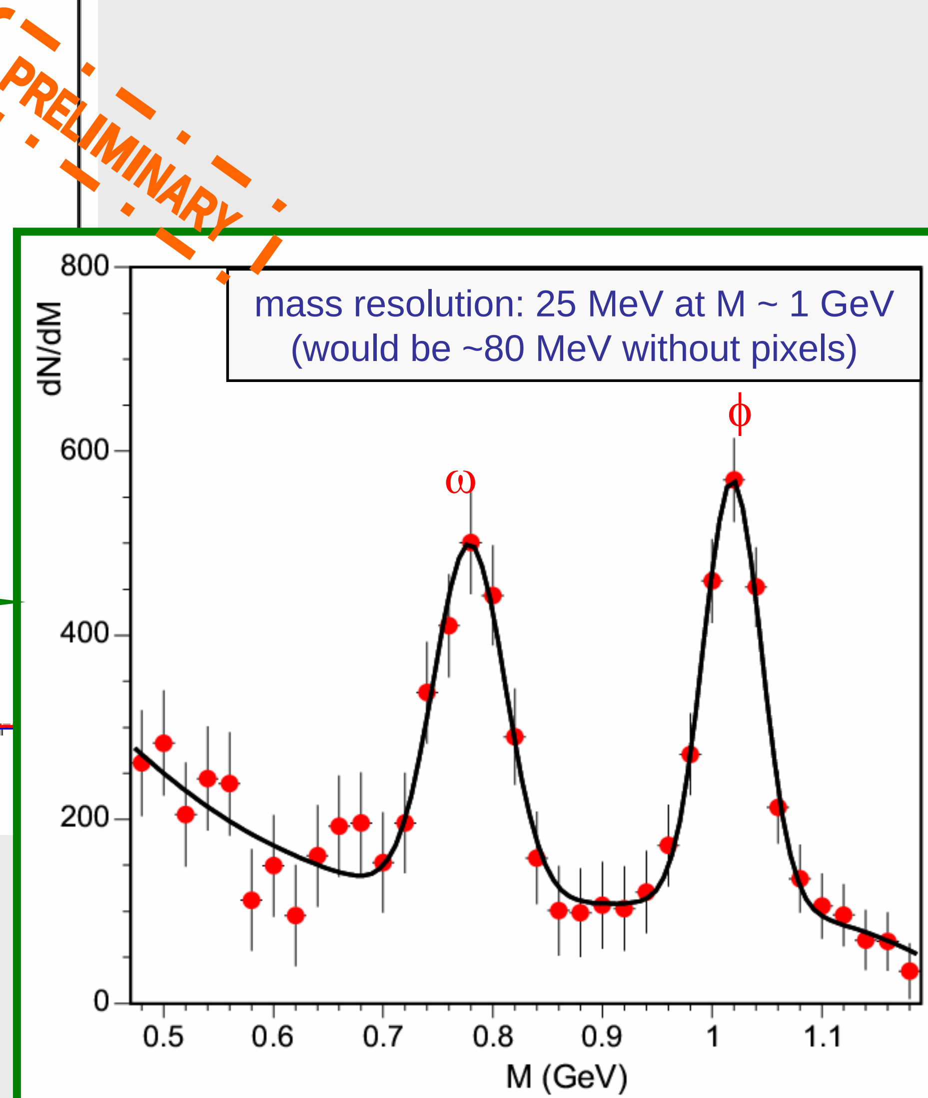

The combinatorial background resulting from π and K decays is estimated through a mixed-event technique, using like-sign muon pairs. The fake matches are not yet included.

The Effects of Radiation in Silicon

- Ionizing Energy Loss (charged particles, photons)
  - transient effect
  - signal creation
- Non-Ionizing Energy Loss (especially hadrons)
  - causes permanent bulk damage
  - depends on particle type, energy ⇒ normalize to 1 MeV n (one 1 MeV neutron equivalent to 2 high-energy hadrons)
  - increases leakage current
  - degrades charge collection efficiency
  - changes effective doping concentration

Fluences in the 2003 Indium-Indium Run

- 5×10^{12} Indium ions on the 20% λ_{int} target during 5 weeks
- Fluences
  - estimated with FLUKA MC simulator
  - measured with Si pin diodes and activation of Al rings during 2 weeks (1.6×10^{12} In ions on target)

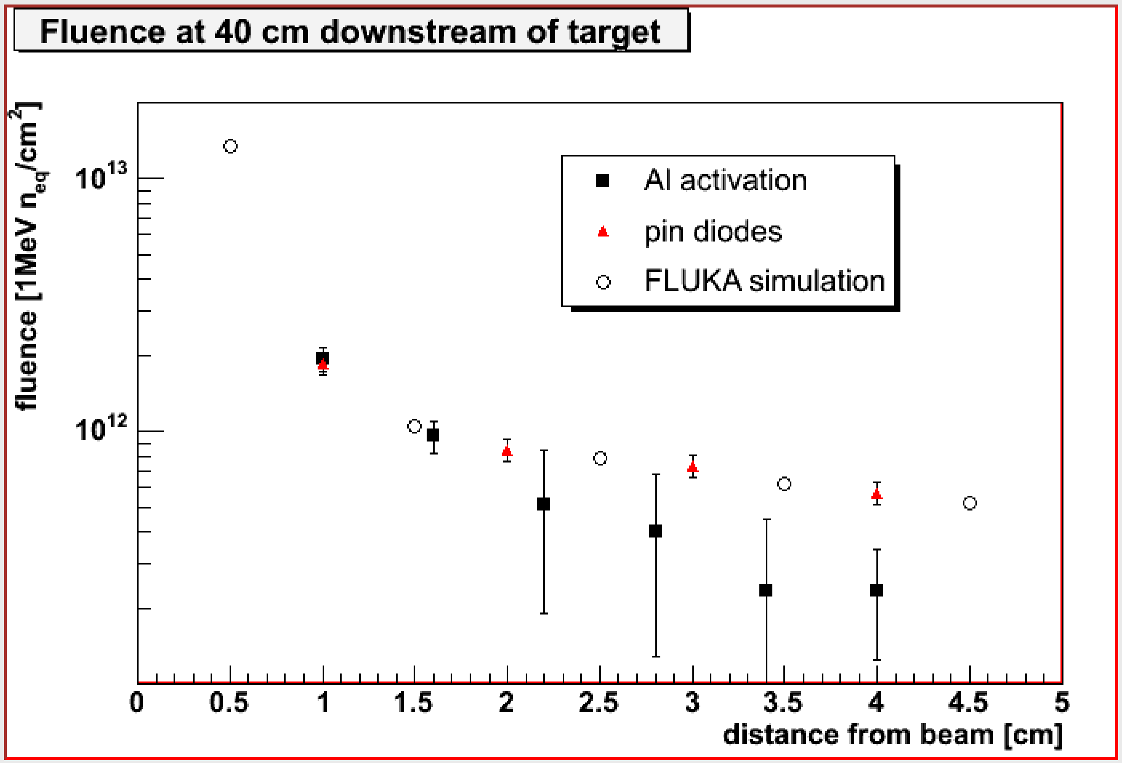

⇒$10^{12} - 5 \cdot 10^{13}$ 1MeV n_{eq}/cm^2 during the 5 weeks, depending on position

Leakage Current

- permanently monitored
- increase proportional to fluence: $\Delta I / V = \alpha \Phi$
- strongly temperature dependent: $I \propto T^2 \exp(-E_{gap} / 2kT)$
  - temperature regulated with cold water cooling
  - temperature monitored with Pt100 sensors

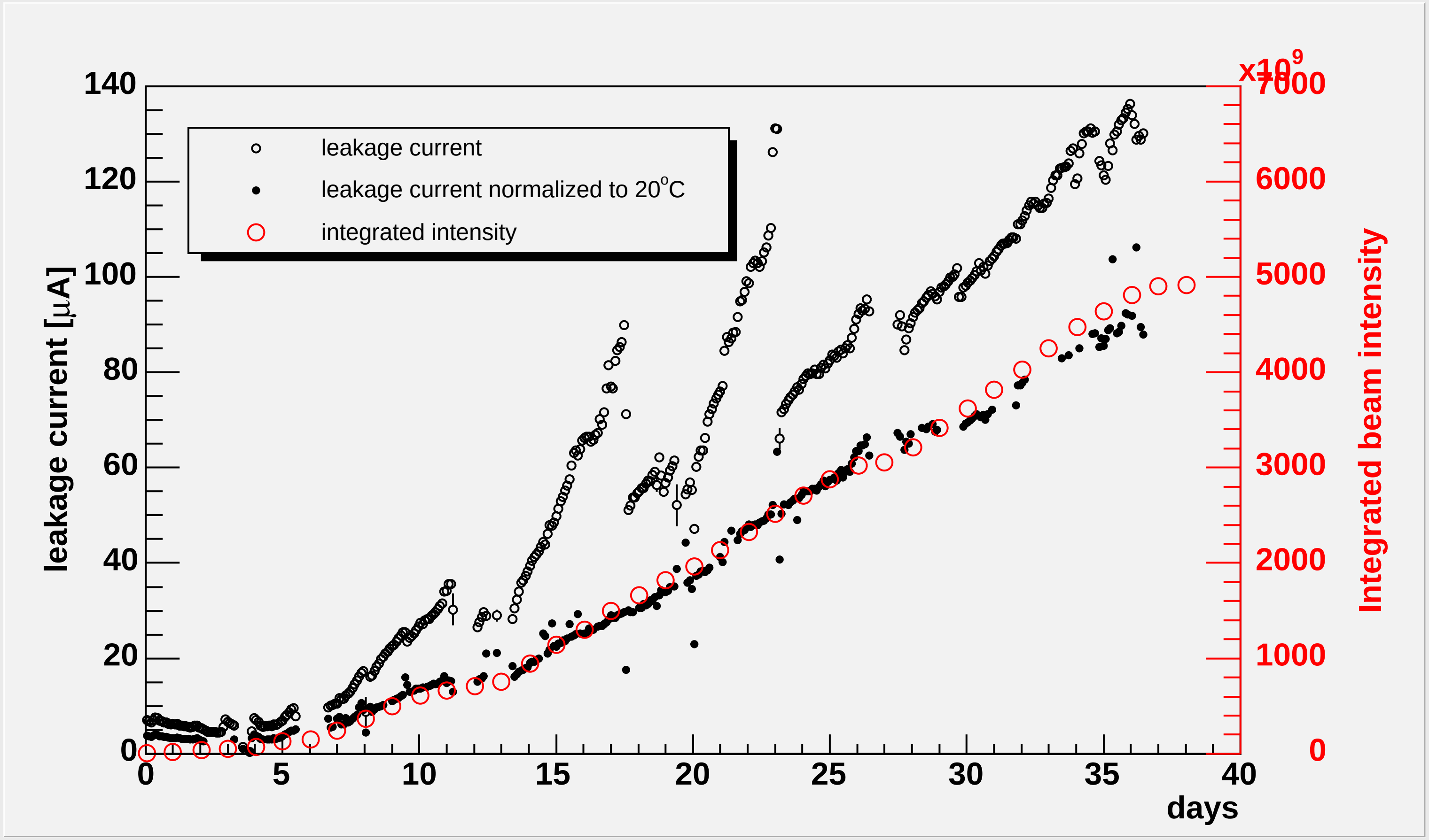

Change in Effective Doping

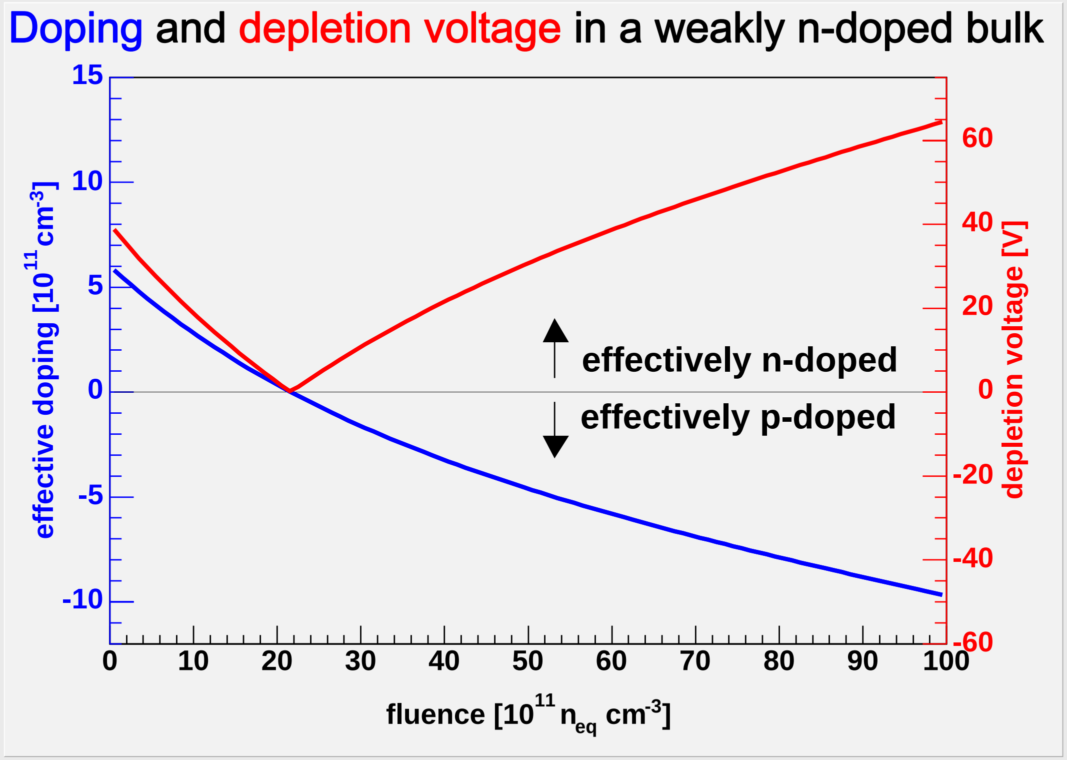

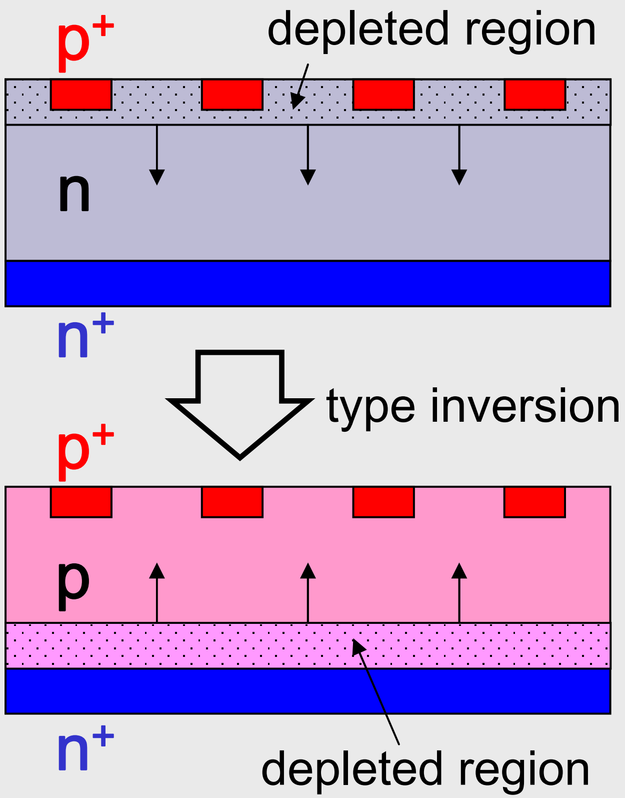

- radiation decreases effective doping concentration in n-type bulk
  - ⇒ bulk eventually becomes effectively p-type (type inversion)
  - ⇒ p-n junction moves from p+ implants to n+ back plane
  - ⇒ full depletion necessary to prevent pixels from being short-circuited
  - ⇒ depletion voltage decreases until type inversion, then increases

Observation of Type Inversion

- pixels at small radii receive more fluence

  ⇒ *after type inversion* expect the depletion voltage to *increase* toward small radii

  ⇒ lowering the bias voltage should leave an ever larger area not fully depleted (i.e. practically dead)

Hit maps taken during a bias voltage scan after 4 weeks

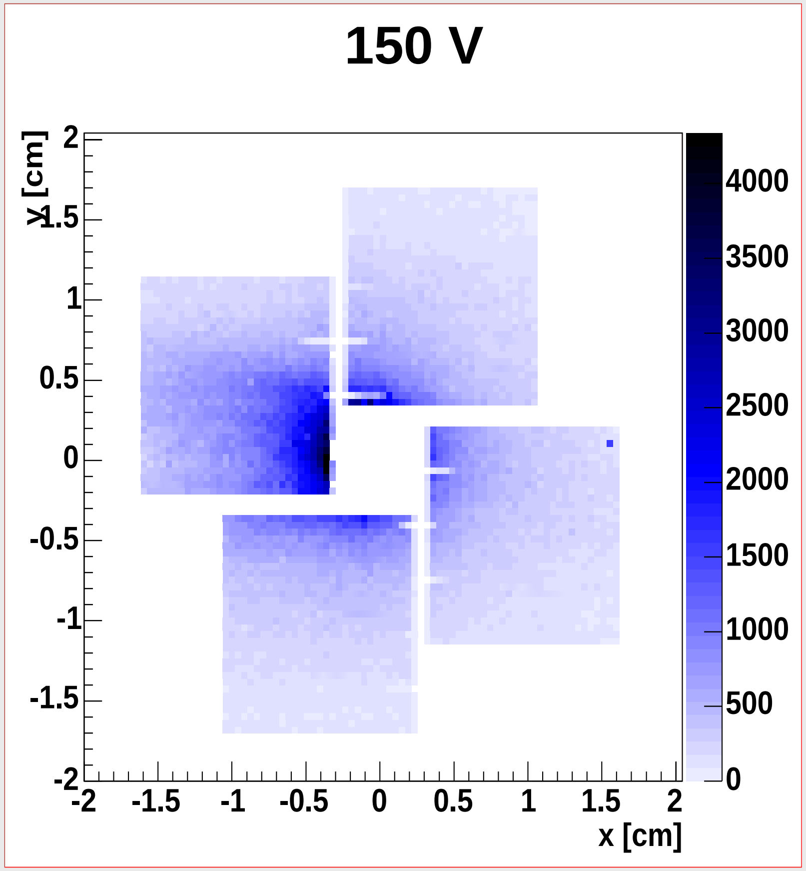

Observation of Type Inversion

- pixels at small radii receive more fluence

  ⇒ *after type inversion* expect the depletion voltage to *increase* toward small radii

  ⇒ lowering the bias voltage should leave an ever larger area not fully depleted (i.e. practically dead)

Hit maps taken during a
bias voltage scan after 4 weeks

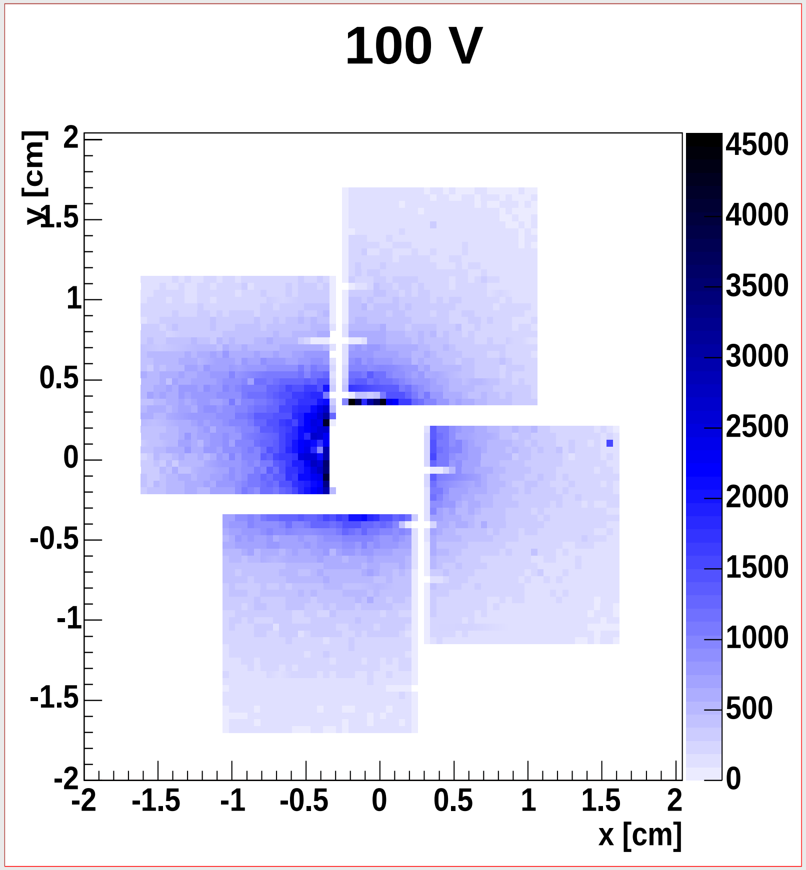

Observation of Type Inversion

- pixels at small radii receive more fluence

⇒ *after type inversion* expect the depletion voltage to *increase* toward small radii

⇒ lowering the bias voltage should leave an ever larger area not fully depleted (i.e. practically dead)

Hit maps taken during a bias voltage scan after 4 weeks

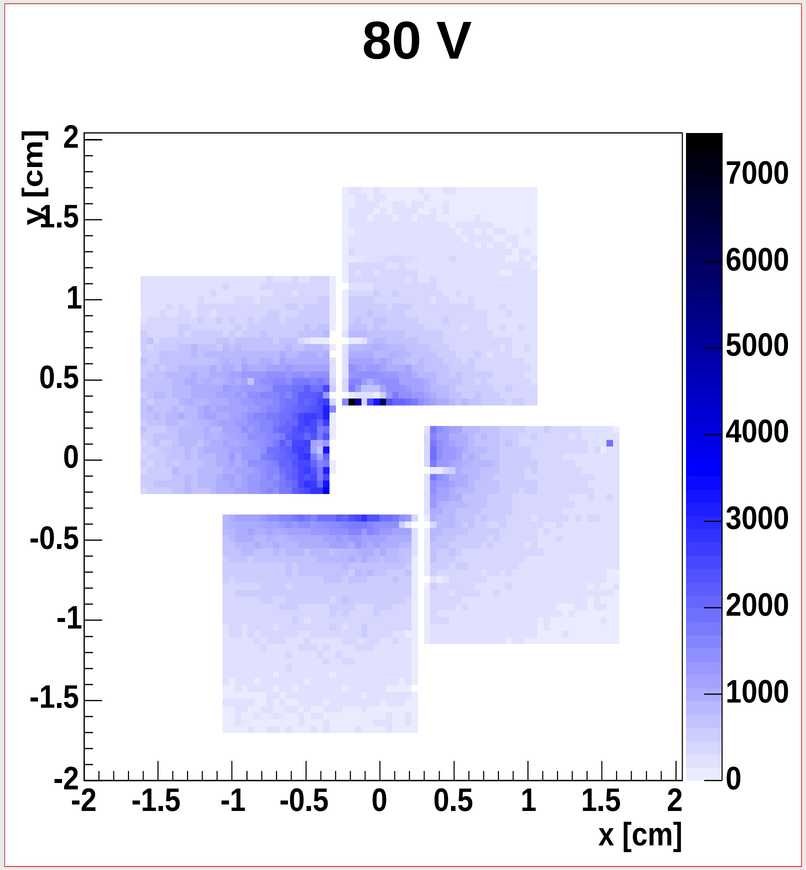

Observation of Type Inversion

- pixels at small radii receive more fluence

  ⇒ *after type inversion* expect the depletion voltage to *increase* toward small radii

  ⇒ lowering the bias voltage should leave an ever larger area not fully depleted (i.e. practically dead)

Hit maps taken during a bias voltage scan after 4 weeks

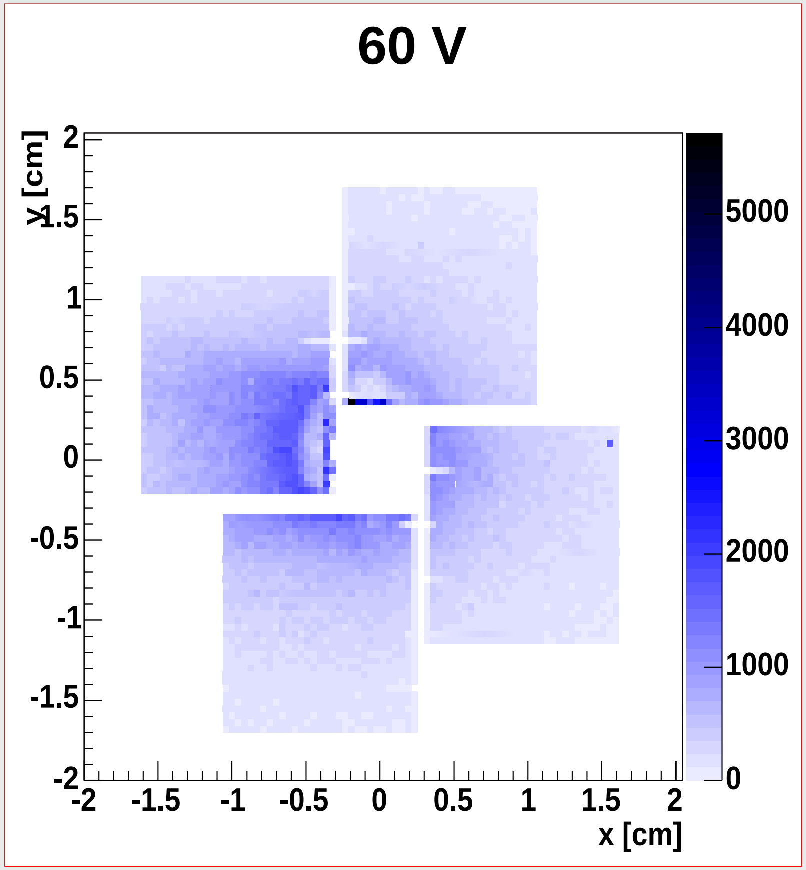

Observation of Type Inversion

- pixels at small radii receive more fluence

  ⇒ *after type inversion* expect the depletion voltage to *increase* toward small radii

  ⇒ lowering the bias voltage should leave an ever larger area not fully depleted (i.e. practically dead)

Hit maps taken during a bias voltage scan after 4 weeks

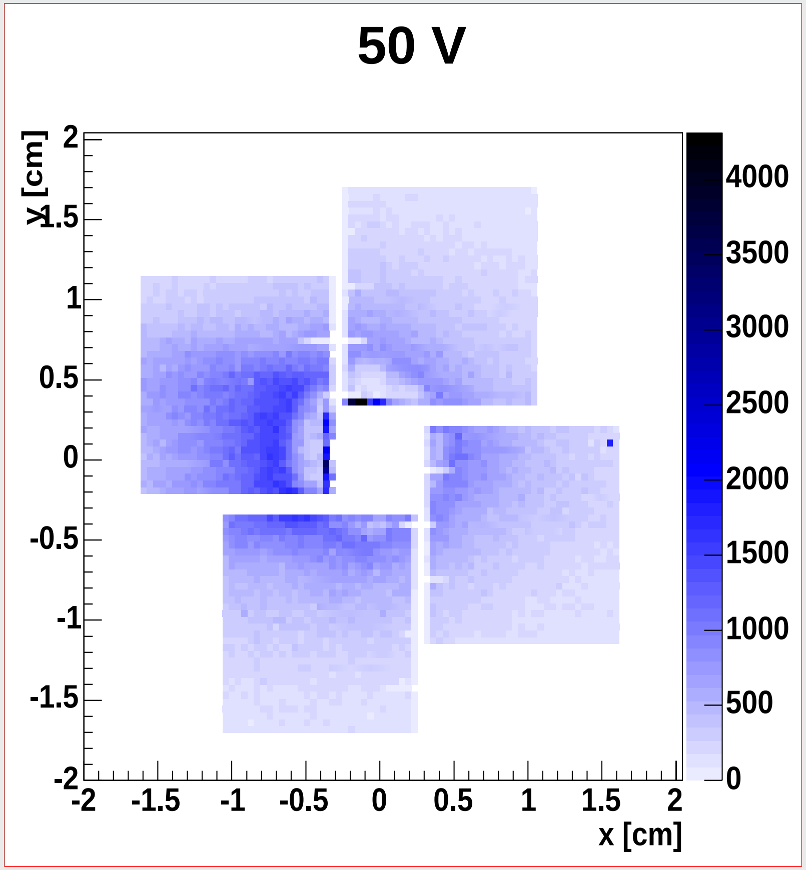

Observation of Type Inversion

- pixels at small radii receive more fluence

  ⇒ *after type inversion* expect the depletion voltage to *increase* toward small radii

  ⇒ lowering the bias voltage should leave an ever larger area not fully depleted (i.e. practically dead)

Hit maps taken during a bias voltage scan after 4 weeks

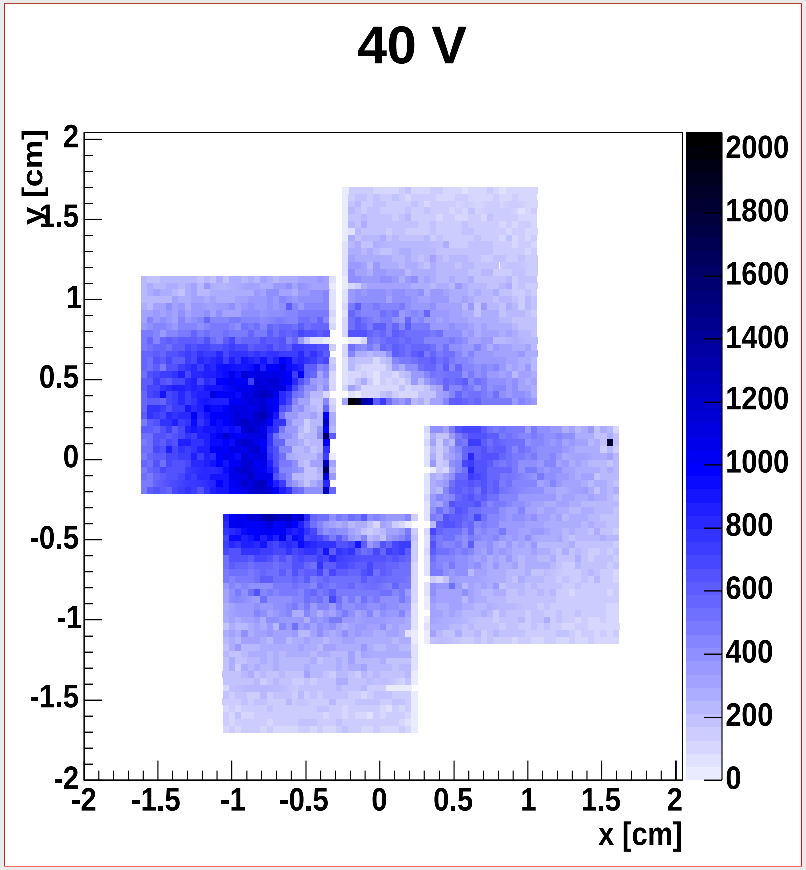

Observation of Type Inversion

- pixels at small radii receive more fluence

  ⇒ *after type inversion* expect the depletion voltage to *increase* toward small radii

  ⇒ lowering the bias voltage should leave an ever larger area not fully depleted (i.e. practically dead)

Hit maps taken during a bias voltage scan after 4 weeks

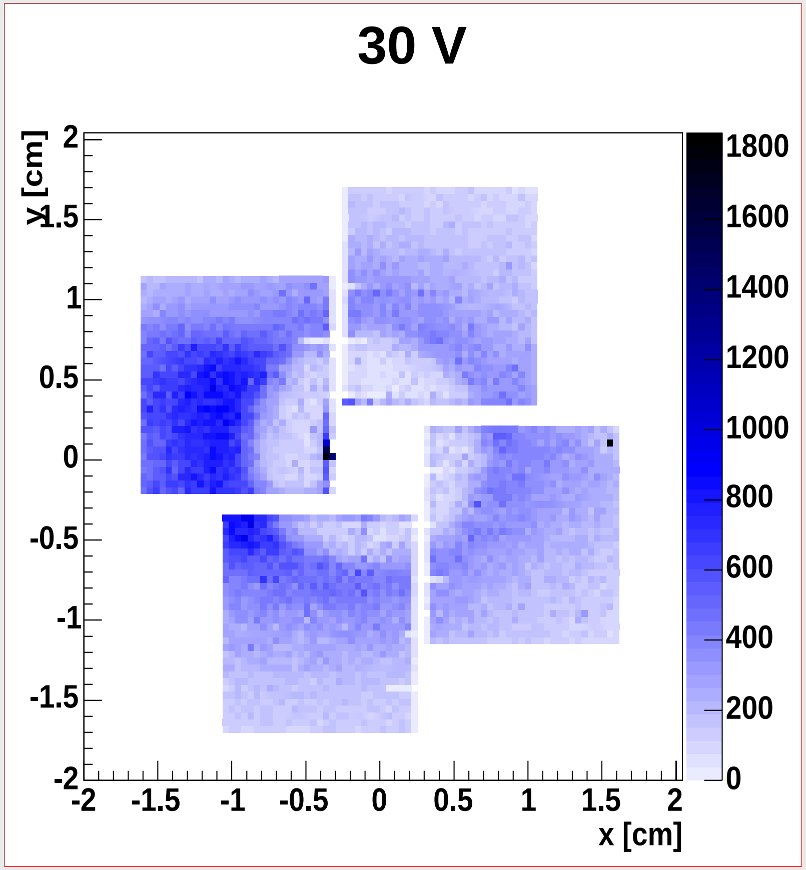

Change of Radiation Damage After Irradiation

- first the damage diminishes (*annealing*)
- after some time the damage increases (*reverse annealing*)
- these effects are strongly temperature dependent

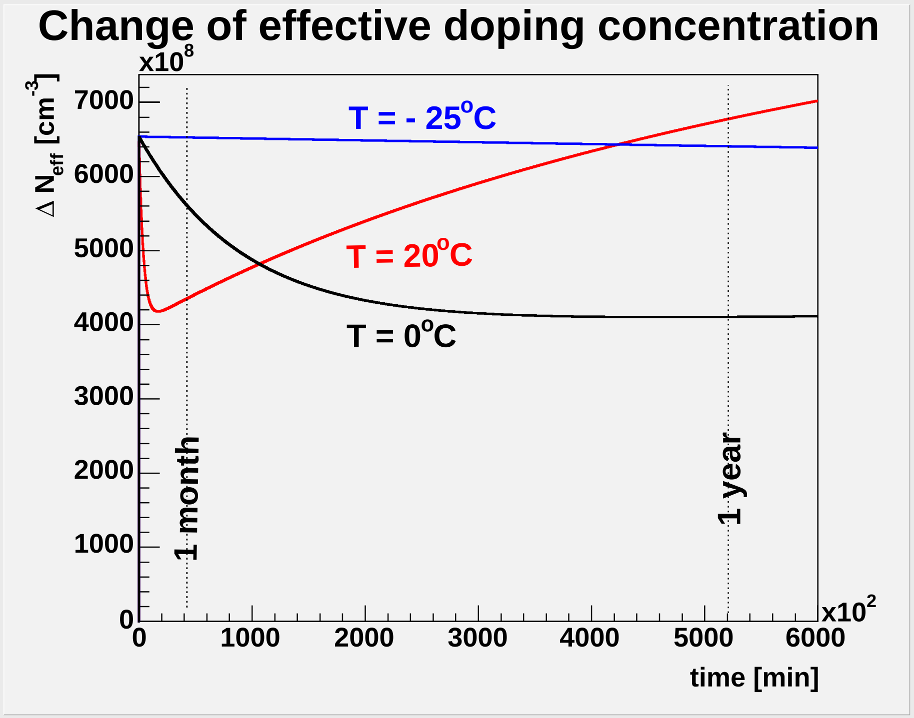

- After the end of run, detector was kept at room T for a month to take full advantage of the beneficial annealing.
- Since then it has been in a freezer at -25 °C to slow down the detrimental reverse annealing.

Summary

- The silicon vertex spectrometer has met the requirements of
  - high speed,
  - high granularity and
  - radiation tolerance

  imposed by the broad and ambitious physics program of NA60.

- Successfully operated a silicon pixel detector in a high-radiation environment for 5 weeks.
  - Detector sustained fluences of 10^{12} to $5 \cdot 10^{13}$ 1MeV n_{eq} / cm^2
  - Effects of radiation damage monitored throughout the run.
  - Predict useful life time to extend half way into this year's proton run.

- Collected in Indium-Indium collisions
  - 1 million low-mass dimuons (after muon track matching)
  - 10^5 J/Ψ events (before muon track matching)

- Analysis of a small sub-sample of the In-In data shows
  - $\sigma_{x,y} \approx 20$ μm and $\sigma_z \approx 300$ μm vertexing precision
  - ~25 MeV mass resolution at ρ and ω

  —unprecedented in fixed-target heavy-ion experiments.

The NA60 Experiment

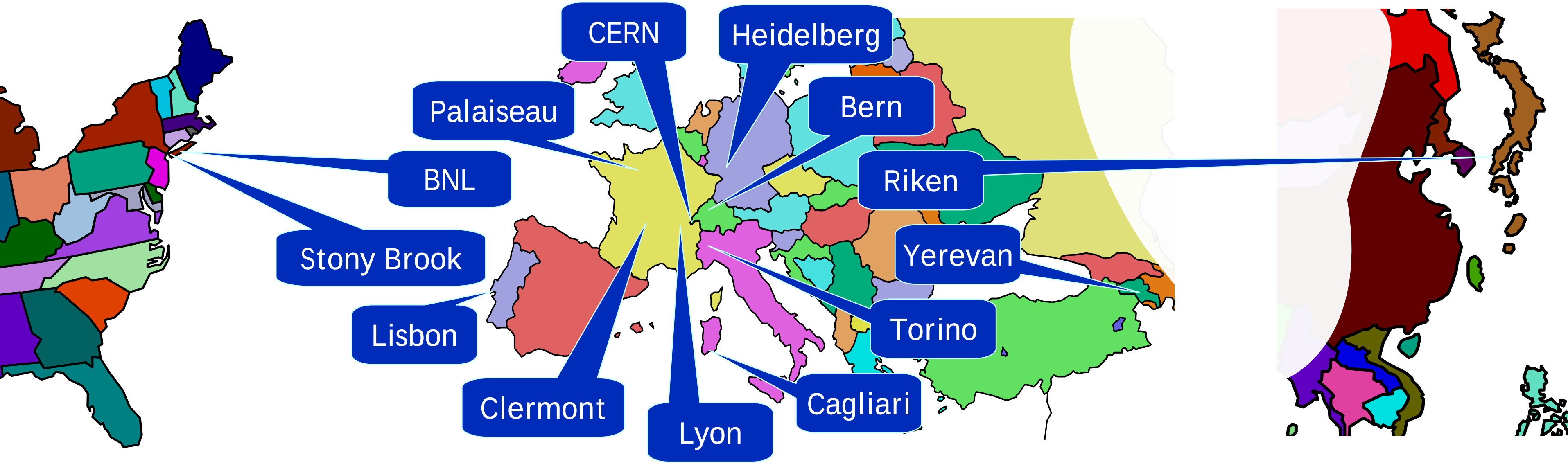

R. Arnaldi, R. Averbeck, K. Banicz, K. Borer, J. Buytaert, J. Castor, B. Chaurand, W. Chen, B. Cheynis, C. Cicalò, A. Colla, P. Cortese, S. Damjanović, A. David, A. de Falco, N. de Marco, A. Devaux, A. Drees, L. Ducroux, H. En'yo, A. Ferretti, M. Floris, P. Force, A. Grigorian, J.Y. Grossiord, N. Guettet, A. Guichard, H. Gulkanian, J. Heuser, M. Keil, L. Kluberg, Z. Li, C. Lourenço, J. Lozano, F. Manso, P. Martins, A. Masoni, A. Neves, H. Ohnishi, C. Oppedisano, P. Parracho, G. Puddu, E. Radermacher, P. Ramalhete, P. Rosinsky, E. Scomparin, J. Seixas, S. Serci, R. Shahoyan, P. Sonderegger, H.J. Specht, R. Tieulent, G. Usai, H. Vardanyan, R. Veenhof, D. Walker and H. Wöhri